



Comparative Tribological and Mechanical Evaluation of Shea Nut Shell and Cow Hoof Reinforced Non-Asbestos Automotive Brake Pads

¹*Haruna, V. N. and ²Sulaiman, I.

¹Mechanical Engineering Department, Federal Polytechnic, Bida, Niger State
haruna.victor@fedpolybida.edu.ng

²Mechanical Engineering Department, Federal Polytechnic, Bida, Niger State
skishk2009@gmail.com

*Corresponding Author: Sulaiman, I.; skishk2009@gmail.com

Manuscript History
Received: 28/08/2025
Revised: 26/11/2025
Accepted: 15/12/2025
Published: 30/12/2025
<https://doi.org/10.5281/zenodo.18355523>

Abstract: The search for sustainable friction materials has intensified following the global phase-out of asbestos in automotive brake pads. This study investigates the potential of shea nut shell (SNS) and cow hoof (CH) powders as locally sourced reinforcements in non-asbestos brake pad composites. Formulations were developed by blending each filler with epoxy resin, graphite, and other conventional additives, followed by compression moulding and post-curing. Specimens were characterized for mechanical properties, tribological performance, and physical behaviour in accordance with ASTM (D3410/D3410M/E-384) and SAE 20/50 standards. Results show that both fillers produced composites with acceptable performance. However, SNS-reinforced samples exhibited lower wear rate, and more consistent friction characteristics, while CH-reinforced composites demonstrated slightly higher density but increased oil absorption. The findings highlight the feasibility of valorising agricultural and animal by-products as eco-friendly brake pad materials, with SNS showing stronger potential for scalable applications. This work contributes to the growing body of research on sustainable, regionally sourced friction composites and offers a pathway for waste valorisation in the automotive aftermarket.

Keywords: Brake Pads, Shea Nut Shell, Cow Hoof, Tribology, Agro-Waste, Sustainable Materials

INTRODUCTION

The composition and characteristics of the friction material greatly influence the performance of brake pads, which are among the most important safety-critical parts of vehicle braking systems (Irwan *et al.*, 2022). Because of their superior heat stability, resistance to wear, and consistent frictional properties, asbestos-based composites have historically dominated the brake pad manufacturing industry (Pradhan *et al.*, 2023). Due to asbestos's carcinogenicity and environmental persistence, it has been outlawed or subject to strict regulations globally, which has increased demand for substitute reinforcements that perform on par with or better. This change has sparked a lot of research into environmentally friendly friction materials made from industrial waste, agricultural residues, and other renewable resources (Curado *et al.*, 2024; Frank, 2020). In non-asbestos brake pad formulations, agro-waste fillers such as groundnut, coconut, rice, and palm kernel shells have shown great promise due to their favourable hardness, low density, and cost advantages (Adeyemi *et al.*, 2024; Nwankwo *et*

al., 2025). Similarly, animal-derived wastes such as bones, horns, and hooves have been studied for their keratinized and mineralized structures, which may contribute to mechanical strength and stability under dynamic braking conditions. The comparative assessment of these two material classes (plant-based and animal-derived fillers) within a single formulation framework has received little attention, despite this expanding body of data ([Issa *et al.*, 2020](#); [Banasaz and Ferraro, 2024](#); [Havlíček *et al.*, 2025](#); [Talabi *et al.*, 2024](#)).

In sub-Saharan Africa, Cow Hooves (CHs) and Shea Nut Shells (SNSs) are examples of abundant yet unused waste streams ([Montcho *et al.*, 2025](#); [Haruna *et al.*, 2019](#)). SNS can be used as thermally stable composite fillers since they are lignocellulosic biomaterials with fixed-carbon content. When handled properly, cow hooves, which are made up of calcium-containing bone fragments and keratin-rich tissue, can contribute structural rigidity and special tribological qualities ([Banasaz and Ferraro, 2024](#); [Ushie *et al.*, 2024](#)). Both materials, if successful, could alleviate the problems associated with environmental waste management while offering inexpensive, locally sourced substitutes for synthetic abrasives and fillers ([Bello and Maladzhi, 2025](#)). In recent years, several studies have explored the development and characterization of eco-friendly, non-asbestos brake friction materials using both agricultural and animal-based wastes, providing useful context for the present work. [Adeyemi *et al.* \(2024\)](#) performed a comparative evaluation of friction materials derived from different agricultural wastes and demonstrated that lignocellulosic fillers such as rice husk and coconut husk offer significant reductions in wear rate while maintaining stable frictional behaviour under elevated temperatures. Their findings highlight the role of plant-based reinforcements in improving thermal and tribological performance, supporting the potential of SNS as a viable filler. Similarly, [Nwankwo *et al.* \(2025\)](#) reviewed the performance characteristics of a wide range of bio-based brake pads and concluded that agro-waste fillers often exhibit favourable hardness-to-density ratios, low thermal conductivity, and reduced specific wear. Their review also emphasized that natural fillers require proper chemical treatment and optimized formulation strategies to achieve interfacial bonding within polymer matrices, aligning with the approach adopted in the present study for SNS and CH powders.

Beyond plant-based fillers, animal-derived reinforcements have also gained attention. [Ushie *et al.* \(2024\)](#) investigated composites reinforced with cow bone and poultry feathers, reporting enhancements in mechanical properties such as tensile and flexural strength due to the mineralized and keratinous nature of the reinforcements. Their findings corroborate observations from other works showing that animal-based materials, when properly processed, can significantly contribute to structural rigidity and wear resistance. This provides evidence supporting the suitability of CH as used in the present study. This study is to provide a comprehensive comparative evaluation of brake pad composites reinforced with powdered CH and SNS, with an emphasis on their frictional performance, wear resistance, thermal stability, and mechanical integrity. Hardness, compressive strength, fade and recovery, wear rate, and coefficient of friction analysis are some of the standardized characterization techniques used in this study to determine performance standards for these materials and evaluate their suitability for large-scale, non-asbestos brake pad manufacturing. It is anticipated that the results would expand the design space for environmentally friendly friction materials and support regional material innovation in the automobile aftermarket.

MATERIALS AND METHODS

2.1 Materials

The selection of materials for this study was informed by their structural relevance, functional roles in friction composite systems, and established performance in prior non-asbestos brake pad formulations. The materials used for this research work include:

- i. Reinforcement materials: SNSs and CHs were the reinforcements used. The SNS were collected from Kodan village in Mokwa Local Government Area of Niger State while the CH was collected from abattoir in Bangaie Area, Bida, Nigeria.
- ii. Binder: Epoxy resin and the hardener were used as the binder to maintain the pad's structural integrity under mechanical and thermal stresses thereby holding the components of the brake pad together and preventing its constituents from crumbling apart.

- iii. Filler: Calcium Carbonate (CaCO_3) was used as the filler material for the purpose of improving manufacturability of the brake pad and reducing its overall cost.
- iv. Graphite rods obtained from used torch light batteries were ground to powder and used as the friction modifier.
- v. Aluminium Oxide (Al_2O_3) obtained from Kaduna was used as the abrasive material. The abrasive is to increase the coefficient of coefficient and to remove iron oxides from the counter friction material as well as other undesirable surface films formed during braking (Umamaheswara *et al.*, 2015).
- vi. Sodium Hydroxide (NaOH) solution having 10 % concentration used to treat the reinforcements was obtained from the same chemical shop where Al_2O_3 was obtained. Distilled water was used to wash away the presence of the NaOH in the treated reinforcements before drying.
- vii. Engine oil (SAE 20/50) was used in carrying out oil absorption test in a similar method adopted by Yawas *et al.* (2016).

2.2 Methodology

The methodology adopted in this study was structured according to established procedures to ensure consistency, accuracy, and reproducibility throughout the experimental investigation.

2.2.1 Preparation of the Reinforcement Materials (Rn)

The SNS and the CH (Fig.1 a and 1 b) collected were each soaked in a solution of water and detergent for 30 minutes for easy removal of dirt and other contaminants. The SNS and CH were thereafter washed properly and sun dried to constant weight after which they were ground using milling machine.

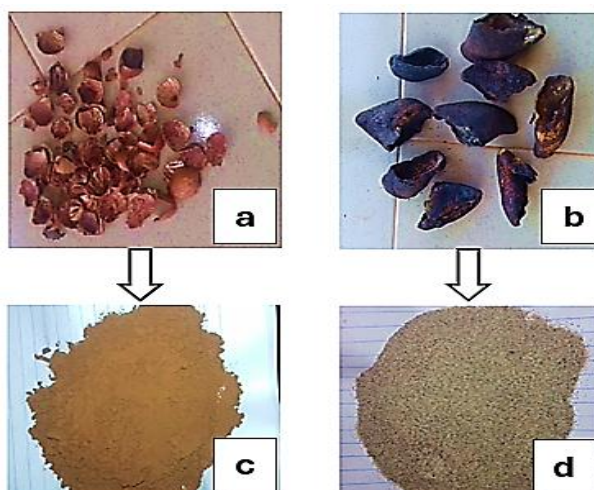


Fig. 1 Milling of SNS and CH, a. SNS, b. CH, c. SNS powder, d. CH powder

The ground reinforcements (Fig. 1 a and 1b) were treated with 10% sodium hydroxide (NaOH) solution and dried for twelve hours until their weights remain constant in a similar method adopted by Abutu (2018). The essence of the chemical treatment of the reinforcements was to modify their surfaces and render them more hydrophobic and more compatible with the resin matrix thus improving the ultimate tensile strength of the developed brake pads (Pujari *et al.*, 2014). The treatment also increases the bonding ability of the reinforcements with the resin (Pujari *et al.*, 2014). These treated reinforcements were then sieved using sieve mesh of 150 μm .

2.2.2 Characterisation of SNS and CH Powders

The compositional analysis was carried out on ground SNS and CH using X-Ray Fluorescence (XRF) machine. XRF analyzers determine the chemistry of a sample by measuring the fluorescent (or secondary) x-ray emitted from a sample when it is excited by a primary x-ray source.

2.2.3 Formulation of the Brake Pad

Formulation of the brake pad samples was done using rule of mixture theorem as adopted by [Abutu et al. \(2018\)](#). In order to use this theorem, the density and volume fraction of each constituent of the brake pad were first determined using a specified weight percent. This specified weight percent used was the composition that gave results that are in close agreement with results from similar research. The volume fraction of the SNS and CH reinforced composites were then calculated using Equation 1 according to [Abutu et al. \(2018\)](#).

$$V_i = \frac{W_i}{\rho_i} \div \sum \frac{W_j}{\rho_j} \quad (1)$$

Where, V_i is the volume fraction of the individual constituent (m^3), W_i is the weight percent of the individual constituent (%), W_j is the weight percent of the total constituents (%), ρ_i is the density of the individual constituent (kg/m^3) and ρ_j is the density of the total constituents (kg/m^3). The volume of the SNS – reinforced composite was calculated using Equation 2.

$$\sum \frac{W_j(s)}{\rho_j} = \frac{W_s}{\rho_s} + \frac{W_g}{\rho_g} + \frac{W_f}{\rho_b} + \frac{W_a}{\rho_a} + \frac{W_m}{\rho_m} \quad (2)$$

Where subscripts s, g, f, a, and m stand for SNS, graphite, calcium carbonate, aluminium oxide and matrix (resin) respectively.

The volume fractions of the individual constituent of CH – reinforced composite were also calculated using Equation 2, except that the subscript 's' was replaced by 'h'. The 'h' stands for cow hoof. The densities of the constituents were determined using Archimedes principle.

2.2.4 Design of Experiment using Taguchi Method

The Taguchi method which combined the design theory experiment and concept of quality loss function involves reducing the variation in a process through robust design of experiments ([Hisam et al., 2024](#)). The design was built in accordance with standard Taguchi's $L_{27}(3)^4$ using Minitab 17 statistical software. [Tables-1](#) and [2](#) show the factor levels of the manufacturing parameters and experimental matrix with control factors respectively.

[Table-1](#) Factor Levels for Manufacturing Parameters

S/N	FACTORS	LEVELS		
1	MP (MPa)	1	2	3
2	MT (°C)	11	13	15
3	Mt (min)	80	90	100
4	PCt (Hour)	7	9	11
		1	1.5	2

Where, MP is the moulding pressure, MT is the moulding temperature, Mt is the moulding time and PCT is the post curing time.

[Table-2](#) Experimental Matrix for Taguchi Design Layout

Run	MP (MPa)	MT (°C)	Mt (min)	PCt (hour)
1	11	80	7	1
2	11	80	7	1
3	11	80	7	1
4	11	90	9	1.5
5	11	90	9	1.5
6	11	90	9	1.5
7	11	100	11	2
8	11	100	11	2
9	11	100	11	2
10	13	80	9	2
11	13	80	9	2
12	13	80	9	2
13	13	90	11	1
14	13	90	11	1

15	13	90	11	1
16	13	100	7	1.5
17	13	100	7	1.5
18	13	100	7	1.5
19	15	80	11	1.5
20	15	80	11	1.5
21	15	80	11	1.5
22	15	90	7	2
23	15	90	7	2
24	15	90	7	2
25	15	100	9	1
26	15	100	9	1
27	15	100	9	1

2.2.5 Production of the Developed Brake Pads

Production of automotive brake pad consists of a number of unit operations including mixing of its components, hot pressing, cooling, post curing and finishing (Muhammed *et al.*, 2024). Powders of the reinforcements, calcium carbonate, graphite and aluminium oxide were thoroughly mixed in a container in the specified weight percentages (Fig. 2). The epoxy (resin + hardener) was properly mixed also in a separate container before being poured into the container containing the first mixture and then mixed thoroughly for five minutes to obtain homogenous mixture.



Fig. 2 Materials for brake pad production: a. Epoxy Resin + Epoxy Catalyst, b. Calcium Carbonate Powder, c. Aluminium Oxide Powder, e. Graphite Rods, f. Graphite Powder

The homogeneous mixture was placed into a metallic mould and compression-moulded using a hydraulic press as shown in Fig. 3. The mould was lined with aluminium foil for easy removal of the cast samples. The mixtures are of the same composition while the manufacturing parameters are varied as shown in Table-2. The final cast products were subjected to post curing process in an electronic oven (Fig. 3) kept at various temperatures and times as also indicated in Table-3. This is similar to the method adopted by Muhammed *et al.* (2024).



Fig. 3 Brake pad production machines

2.2.5 Moulds Preparation

Three different moulds made from mild steel were used in the course of producing the brake pad samples. Two of the moulds having dimensions $100 \times 80 \times 5$ mm and $100 \times 80 \times 10$ mm were used in producing the samples from which specimens for various tests were cut. The third mould having a dimension of $200 \times 170 \times 5$ mm was used to produce the optimized brake pad samples. The moulds were produced by first marking out the dimensions of the respective moulds on the mild steel plate using steel rule and scribe. Electric hand grinding machine was then used to remove the unwanted parts of the plate and finally dressing the moulds to their required shapes. The developed SNS and CH brake pads are presented in Fig. 4.



Fig. 4 Developed CH and SNS Reinforced Brake Pad Samples

2.2.6 Water and Oil Absorption Tests

The 24-hour water and oil soak tests were carried out to determine the water and oil absorption behaviour of the brake pads produced. The samples were oven dried at 70°C for one hour and their weights measured using digital weighing machine. After twenty-four hours of submersion in water and engine oil (SAE 20/50) at 30°C , the specimens were weighed again after the excess water and oil had drained off. This is in accordance with the method adopted by [Akincioğlu *et al.* \(2021\)](#). The absorptions were calculated using Equation 3 ([Akincioğlu *et al.* \(2021\)](#)).

$$\text{Absorption}(\%) = \frac{W_1 - W_0}{W_0} \times 100\% \quad (3)$$

Where W_1 is the weight after immersion in (g) and W_0 is the weight before immersion (g).

2.2.7 Compression Test

Three specimens were provided for each sample and subjected to compressive test using Enerpac Universal Hydraulic Digital Material Testing Machine 100KN, Norwood Instrument shown in Fig. 5 in accordance with ASTM D3410/D3410M ([Morăraș *et al.*, 2024](#)). The specimens were cut to a dimension of $20 \times 20 \times 10$ mm in order to conform to the specification of the instrument used. These specimens were loaded continuously until failure occurs.



Fig. 5 Compression Testing Machine

2.2.8 Hardness Test

Hardness was carried to determine resistance to indentation in accordance with ASTM E-384 in using Digital Micro Vickers Hardness Tester, HVC – 30E (Fig. 6). The specimen specification of the tester is $20 \times 20 \times 10$ mm. The test was carried out at three different points for each specimen and the average value was recorded which is similar to the method adopted by [Saraki et al. \(2025\)](#). It is an optical method in which the size of indentation left by the indenter is measured to determine the hardness value of the specimen. The larger the indent left by the indenter, the softer the material tested. The indenter is an equilateral pyramid with a square base made of diamond with a plane angle of 136° .



Fig. 6 Hardness Testing Machine

2.2.9 Wear Rate

Wear rate test was conducted in two parts. The first part was carried out on the Taguchi experimental design samples produced in accordance with ASTM D4966-98 standards ([Abutu et al., 2018](#)). This was carried out using Martindale Abrasion Testing Machine (SATRA TECHNOLOGY, S/N 11884, STM: 105, supply – 230-1-50) operating at a speed of 50 rev/min (Fig. 7). Attached to the machine was a stainless steel disc of 135 mm diameter coated with a detachable fabric material mounted on each disc of the machine to serve as the abradant. The prepared specimen having a diameter of 38 mm and thickness of 5 mm was subjected to abrasion test for a cycle of 1000 in 1200 s at a pressure of 1.26 MPa and at constant speed of 50 rev/min. At the end of the test, the specimen and the abraded particles on the surface of the abradant were removed the wear rate, weight loss, sliding distance, wear index, wear cycle and abrasion resistance determined respectively.



Fig. 7 Martindale Abrasion Machine

The second part of the wear test was carried out using the Tribometer (Fig. 8), Anton Paar, Switzerland to investigate the dry sliding wear rate and coefficient of friction of the samples in accordance with ASTM G99 – 05 standards (Idris *et al.*, 2015). The samples dimensions were 25 mm in diameter and 5 mm in thickness. The result of the wear test using this apparatus was displayed on the screen of the computer attached to it.



Fig. 8 Tribometer

2.2.10 Coefficient of Friction Test

This test was carried out in accordance with the procedure recommended by Abutu *et al.* (2018). The procedure involved cleaning the surfaces of the inclined plane and the specimen with a dry cloth to avoid any unwanted particle that may be on the inclined plane and the specimen. The inclined plane was then set to a fixed angle (θ). In this work, the angle used was 15° . The specimen was then attached to the base of a slider made of mild steel plate using super glue to prevent it from falling off when conducting the test. The weight of the specimen together with the slider was measured using electronic digital weighing machine before placing it on the inclined plane. A weighing hanger of 5 N was attached to the hook on the slider via a cord. The load on the weight hanger was gradually increased until the specimen is at verge of sliding up the surface of the inclined plane and the load at this was recorded. These steps were repeated to determine the coefficient of friction of all the specimens.

2.2.11 Thermal Conductivity Test

Thermal conductivity, k is the property of a material that indicates its ability to conduct heat. Conduction will take place if there is existence of temperature gradient in a solid. This test was conducted using Searle's apparatus (Fig. 9). The specimen can be in cylindrical or rectangular form similar to the method adopted by Ademoh and Olabisi (2015). However, the specimens in this research work are in rectangular form. One end of the specimen goes into the steam chamber while a copper tube is coiled around the other end. Water enters the tube at the end away from the steam chamber and leaves at the end nearer to it. Thermometers T_3 and T_4 are provided to measure the temperatures of the outgoing and incoming water. Two holes are drilled in the rod and mercury is filled in these holes to measure the temperatures of the specimen at these places with the help of thermometers T_1 and T_2 . Steam is passed into the steam chamber, and a stream of water is maintained. The temperatures of the entire four thermometers rise initially and ultimately become constant when the steady state is reached and the readings are recorded. The whole apparatus is covered properly with layers of an insulating material to prevent loss of heat to the surrounding environment. The entire set up consists of the Searle's apparatus, four thermometers, water base, power source, ammeter and voltmeter.



Fig. 9 Searle's Apparatus

2.2.12 Thermo-gravimetric Analysis

The samples were subjected to thermo-gravimetric analyses (TGA) to determine their thermal stability using Thermo-gravimetric Analyzer. The analyzer detects the mass loss of the respective samples as a function of temperature (Ruzaidi *et al.*, 2011). The samples were evenly and loosely distributed in an open sample pan of 6.4 mm diameter and 3.2 mm deep with an initial sample of 10 - 14 mg. the temperature change was controlled from 30 °C to 950 °C at a heating rate of 10 °C/min. nitrogen was continuously passed through the furnace at a flow rate of 60 mL/min at room temperature and atmospheric pressure. Before initiating each run, nitrogen was used to purge the furnace for 30 minutes to establish inert environment to stop any occurrence of oxidative decomposition. The TG and DTA curves were obtained from TGA runs using universal analysis 2000 software from TA instrument.

RESULTS AND DISCUSSION

This section presents the findings of the study and provides an analytical interpretation of the experimental outcomes.

3.1 Characterization of the SNS and CH

The knowledge of the elemental compositions helps to establish the acceptance of the reinforcements as candidates or materials to be used in the production of brake pads. Table-3 shows the percentage composition of the elements in the reinforcements.

Table-3 Chemical Analysis of SNS and CH

Elemental Composition	SNS (%)	CH (%)
Si	12.00	0.73
K	17.00	10.00
Ca	8.10	31.00
Ti	2.50	N/D
Ni	0.30	N/D
Mn	0.30	N/D
Fe	19.70	2.45
Cu	0.70	0.78
Zn	N/D	0.69
C	28.60	21.50
Na	4.10	3.40
Mg	1.10	1.00
As	0.39	0.90
Pb	0.88	0.06
S	4.00	17.50

N/D = Not Detected

Chemical compositions of various types of asbestos are shown in Table-4.

Table-4 Chemical Composition of Various Types of Asbestos (Croce *et al.*, 2023)

Element (%)	Chrysotile	Crocidolite	Amosite	Anthophyllite	Tromolite
SiO ₂	37-44	49-53	49-53	50-58	51-62
MgO	39-44	0-3	1-7	28-34	0-30
FeO	0-6	13-20	34-44	3-12	1.5-5
Fe ₂ O ₃	0.1-5	17-20	-	-	-
Al ₂ O ₃	0.2-1.5	-	2-9	0.5	1-4
H ₂ O	12-15	2.5-4.5	2-5	1-6	0.5
CaO	0-5	-	-	-	0-18
Na ₂ O	-	4-8.6	-	-	0-9
CaO+Na ₂ O	-	-	0.5-2.5	-	-

The result in [Table-3](#) shows that silicon, potassium, calcium, titanium, iron, carbon, sodium, magnesium and sulphur are the major constituents of SNS, while CH has its major constituents as potassium, calcium, iron, carbon, sodium, magnesium and sulphur. However, some other elements were found to be present in traces. The presence of hard elements like silicon, calcium, iron, carbon and magnesium which are equally found in asbestos (See [Table-4](#)) suggests that SNS and CH particles can be used as filler materials for brake pad production as similarly observed by [Adekunle et al. \(2023\)](#).

3.2 Brake Pad Formulation using Rule of Mixture

Summary of the brake pad composition formulated using rule of mixture theorem is shown in [Table-5](#).

[Table-5](#) Summary of the Formulation of the Brake Pad Composition

SNS- Reinforced Brake Pad					CH- Reinforced Brake Pad				
Constituent	V _i	W _i	Mass	ρ	Constituent	V _i	W _i	Mass	ρ
		(%)	(g)	(g/cm ³)			(%)	(g)	(g/cm ³)
M	0.0955	25	43.97	2.63	M	0.1143	25	43.97	2.63
S	0.4111	25	43.99	0.611	H	0.2953	25	43.99	1.018
F	0.2975	30	52.78	1.013	F	0.3561	30	52.78	1.013
G	0.0963	10	17.59	1.043	G	0.1153	10	17.59	1.043
A	0.0996	10	17.6	1.009	A	0.1192	10	17.6	1.009
Total	1.000	100	176	1.005	Total	1.0000	100	176	1.203

M = matrix, S = SNS, H = CH, F = CaCO₃, G = Graphite, A = Al₂O₃

The formulation of the brake pads in [Table-5](#) shows that the SNS-reinforced brake pad with predicted density of 1.005 g/cm³ will be less dense than the CH-reinforced brake pad which is having predicted density of 1.203 g/cm³ when produced. This may be as a result of the greater value of the density of the pulverized CH than the value of the density of the pulverized SNS. It can also be concluded that the predicted values obtained from the results are in close agreement with the recommended values of commercial asbestos brake pad that has density values ranging from 1.01 – 2.06 g/cm³ as reported by [Adekunle et al. \(2023\)](#); [Ikpambese et al. \(2014\)](#); [Abutu et al. \(2018\)](#) and [Abutu et al. \(2019\)](#). The mass of the brake pad samples in this research work is targeted at 176 g which is the mass of the commercial asbestos brake pads as reported by [Ikpambese et al. \(2014\)](#).

3.3 Water Absorption Test

The results of the water absorption test for SNS and CH reinforced brake pad samples are shown graphically in [Fig. 10](#). The water absorption rate of the brake pad samples changes with variation in the manufacturing parameters. The water absorption rate of SNS-reinforced samples varied from 0.0159 % to 0.0633 % while that of CH-reinforced samples range from 0.0364 % to 0.1050 %. The highest being that of sample 12 for CH as indicated in [Fig. 10](#).

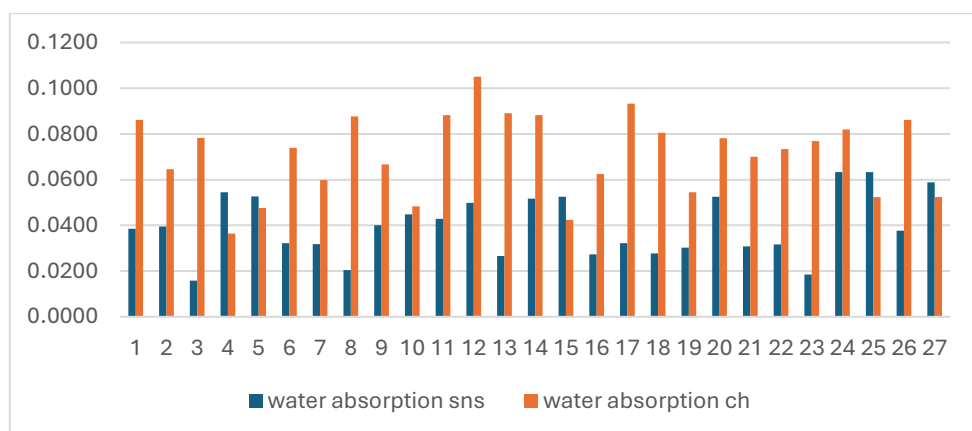


[Fig. 10](#) Water Absorption Rate of the Brake Pad Samples

This indicates that the SNS-reinforced samples have lower values of absorption rate compared to CH-reinforced samples across all samples examined. These lower values of absorption rate in SNS-reinforced samples may be attributed to decreased pores resulting from distribution of resin and close interfacial packing (Blau, 2001; Dagwa and Ibhadode, 2005).

3.4 Oil Absorption Rate

Experimental results of the oil absorption rate of the developed brake pad samples are displayed in Fig. 11. The oil absorption rate of SNS-reinforced samples ranges from 0.0256 % to 0.0909 % while that of CH-reinforced samples ranges from 0.0523 % to 0.1225 %.

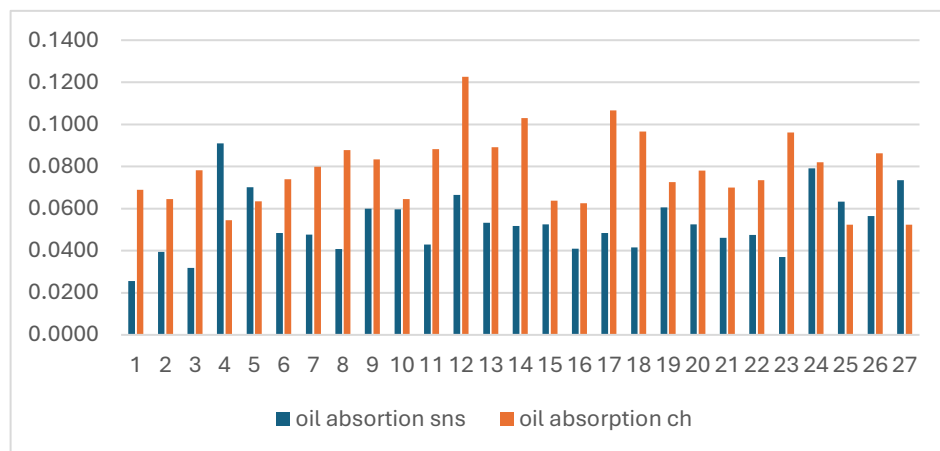


Fig. 11 Oil Absorption Rate of the Brake Pad Samples

Sample 12 of CH also has the highest value. The sample is having MP of 13 MPa, MT of 80 °C, Mt of 9 minutes and PCT of 2 hours. This means that the SNS-reinforced samples have lower values of oil absorption rate as compared to CH-reinforced samples. It can also be observed from the figure that the oil absorption rate changes with variation in the manufacturing parameters. CH particles exhibit a higher oil absorption rate than SNS because their keratin-based structure is more porous and hydrophobic, allowing oil to penetrate and adhere more readily as stated by Bala *et al.* (2016). In contrast, SNS are dense and lignocellulosic, with smoother surfaces that limit oil uptake (Mbakbaye *et al.*, 2021; Zievie *et al.*, 2024; Bala *et al.*, 2016).

3.5 Compressive Test

Fig. 12 depicts the results of the compressive test carried out on the developed brake pad samples. Samples 18 and 12 of CH-reinforced samples have the highest and lowest values of 85.52 MPa and 41.7 MPa respectively. These results indicate that the SNS-reinforced brake pad has a better ability to withstand compressive stress. This better compressive strength may be as a result of increase in surface area and pore packaging capability (Aigbodion *et al.*, 2010).

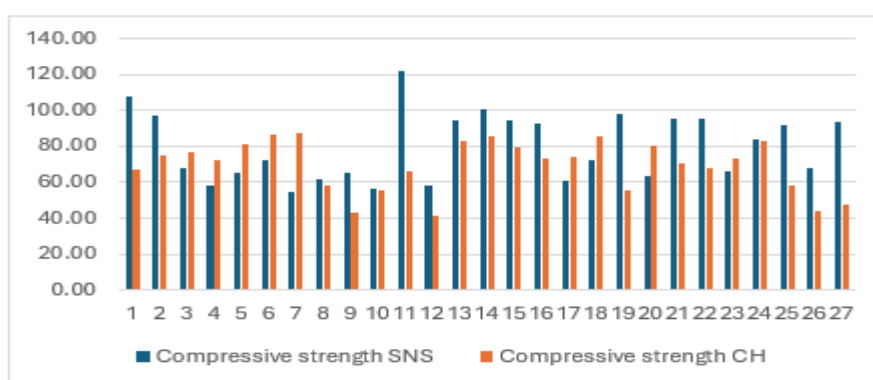


Fig. 12 Compressive Strength of the Brake Pad Samples

The reinforced brake pad with SNS exhibit higher compressive strength because the dense, rigid lignocellulosic particles improve load-bearing capacity within the composite matrix (Haruna *et al.*, 2019). This is also inferred from the oil absorption rate being lower due to the lower porosity of the SNS.

3.6 Hardness Test (Vickers)

Fig. 13 shows that the hardness value of the brake pad samples changes with variation in the manufacturing parameters. The hardness value of SNS-reinforced brake pad samples varied from 17.8 to 42.5 while the CH-reinforced samples varied from 10.6 to 42.73.

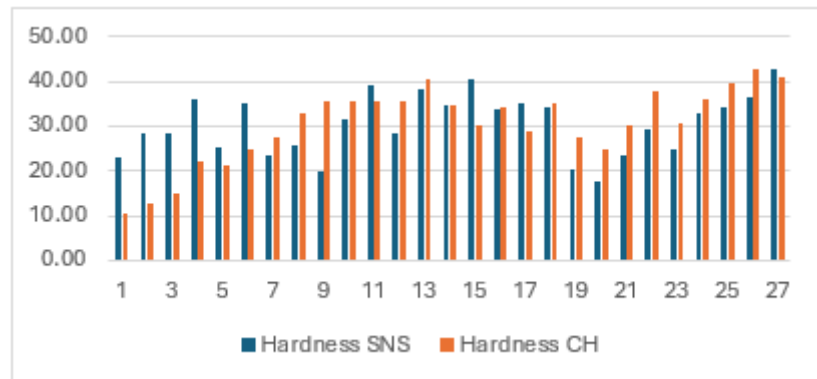


Fig. 13 Hardness Value of the Brake Pad Samples

The SNS-reinforced and CH-reinforced samples are having almost the same highest hardness value of 42.5 and 42.73 respectively. This means that both reinforced samples are having about the same ability to withstand plastic deformation. Better hardness values may be attributed to increase in surface area which resulted to increase in bonding ability with the resin (Ushie *et al.*, 2024; Aigbodion *et al.*, 2010). The hardness may be as a result of closer packing of the particles thereby creating more homogeneity in the entire phase of the composite body (Dagwa and Ibhadode, 2006).

3.7 Wear Rate Test

Fig. 14 shows that the wear rate of the brake pad samples changes with variation in the manufacturing parameters.

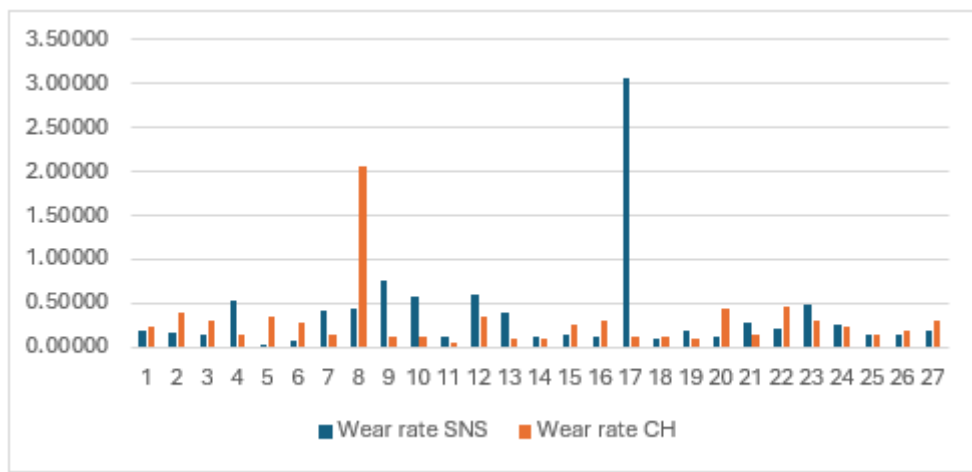


Fig. 14 Wear Rate of the Brake Pad Samples

The wear rate of SNS-reinforced brake pad samples varied from 0.03929 mg/m to 3.06481 mg/m while the CH-reinforced samples varied from 0.05894 mg/m to 2.0628 mg/m. It can be observed that the SNS-reinforced brake pad samples have the lowest wear rate of 0.0393mg/m.

3.8 Coefficient of Friction Test

Fig. 15 shows that the coefficient of friction of the brake pad samples changes with variation in the manufacturing parameters. The values of the coefficient of friction of SNS-reinforced brake pad samples range from 0.565 to 0.868 and from 0.631 to 0.877 for CH-reinforced brake pad samples (Ekpruke *et al.*, 2023). These values are within the class H ($\mu > 0.55$) type of brake pads recommended by the Society of Automobile Engineers (SAE) for use in automobiles (Adetunji *et al.*, 2022).

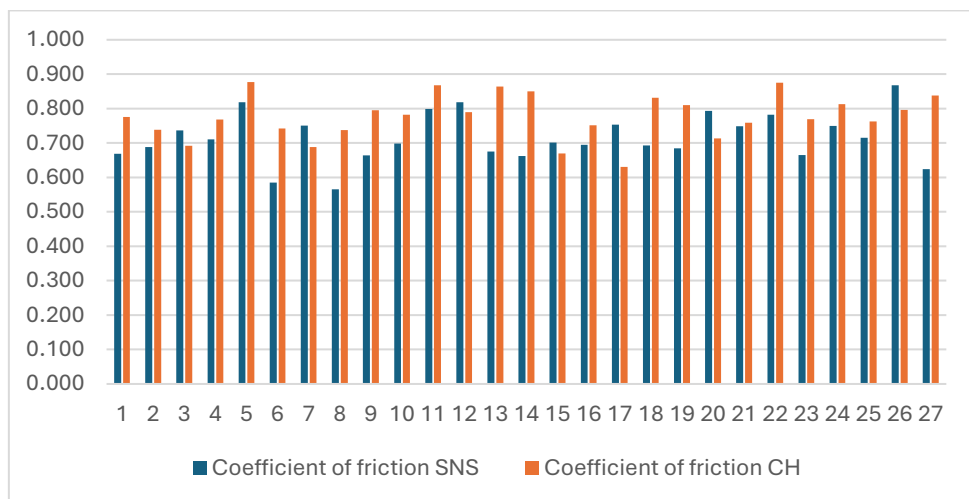


Fig. 15 Coefficient of Friction of the Brake Pad Samples

This was also reported by Blau, (2001) and Dagwa and Ibhadode (2006). Therefore, both the SNS and CH-reinforced brake pads are suitable for use in both light and heavy duty automobiles. These results indicate that CH-reinforced samples have higher value of coefficient of friction than the SNS-reinforced samples.

CONCLUSION

This study has demonstrated that both SNS and CH powders possess the elemental characteristics required for effective friction materials in non-asbestos automotive brake pad production. The presence of hard constituents such as silicon, calcium, iron, carbon and magnesium supports their suitability as reinforcing fillers. The predicted density values of the developed SNS- and CH-based composites fall within the established range for commercial asbestos brake pads (1.01–2.06 g/cm³), further confirming their compatibility with existing industry standards. Performance evaluation revealed that SNS-reinforced composites consistently exhibited lower water and oil absorption rates than CH-based samples, a behaviour attributed to reduced porosity and improved resin distribution within the SNS matrix. SNS reinforcement also produced brake pads with superior compressive strength, indicating enhanced load-bearing capacity. Hardness results showed that both SNS and CH composites possess comparable resistance to plastic deformation. Tribological analysis established that all developed samples satisfy the SAE Class H friction requirement ($\mu > 0.55$), confirming their applicability in both light- and heavy-duty automotive braking systems. Although SNS demonstrated lower wear and absorption tendencies, CH-based specimens exhibited slightly higher coefficients of friction, which may be advantageous in applications requiring increased braking response.

Overall, the findings validate SNS and CH as viable, sustainable alternatives to asbestos in brake pad formulation, with SNS showing stronger potential due to its superior mechanical and absorption characteristics, and CH offering acceptable performance with enhanced frictional response.

CONFLICT OF INTEREST

The authors declare that there is no conflict of interest regarding the publication of this paper.

REFERENCES

Abutu, J., Lawal, S. A., Ndaliman, M. B., Lafia-Araga, R. A., Adedipe, O., & Choudhury, I. A. (2018). Effects of process parameters on the properties of brake pad developed from seashell as reinforcement material using grey relational analysis. *Engineering Science and Technology, an International Journal*, 21(4): 787-797.

Abutu, J., Lawal, S. A., Ndaliman, M. B., Lafia-Araga, R. A., Adedipe, O., & Choudhury, I. A. (2019). Production and characterization of brake pad developed from coconut shell reinforcement material using central composite design. *Springer Nature Journal of Applied Sciences*, 1(82), 1-15.

Adekunle, A., Okunlola, M., Omoniyia, P., Adeleke, A., Ikubanni, P., Popoola, T., & Ibrahim, H. (2023). Development and analysis of friction material for eco-friendly brake pad using seashell composite. *Scientia Iranica*, 30(5), 1562-1571.

Adekunle, N. O., Ismaila, S. O., Kuye, S. I., Adetunji, R., Olamide, O. O., & Tomori, O. (2023). Design and production of asbestos free brake pad using cashew nutshell. *LAUTECH Journal of Engineering and Technology*, 17(1), 8-17.

Ademoh, N. A., & Olabisi, A. I. . (2015). Development and evaluation of maize husks (asbestos – free) based brake pad. *Industrial Engineering Letters*, 5(2): 67 – 80.

Adetunji, O. R., Adebayo, A. M., Ismaila, S. O., Dairo, O. U., Okediran, I. K., & Adesusi, O. M. (2022). Effect of silica on the mechanical properties of palm kernel shell based automotive brake pad. *Mechanical Engineering for Society and Industry*, 2(1), 7-16.

Adeyemi, O. I., Kirwan, K., Tuersley, I., & Coles, S. R. (2024). Comparative assessment of the performance of friction materials based on different agricultural wastes. *Tribology International*, 191(1), 1-15.

Aigbodion, V. S., Akadike, U., Hassan, S. B., Asuke, F., & Agunsoye, J. O. . (2010). Development of asbestos – free brake pad using bagasse. *Tribology in Industry*, 32(1), 45 – 50.

Akincioglu, G., Akincioglu, S., Oktem, H., & Uygur, I. (2021). Brake pad performance characteristic assessment methods. *International Journal of Automotive Science and Technology*, 5(1), 67-78.

Bala, K. C., Okoli, M., & Abolarin, M. S. (2016). Development of automobile brake lining using pulverized cow hooves. *Leonardo Journal of Sciences*, 28(8), 95-108.

Banasaz, S., & Ferraro, V. (2024). Keratin from animal by-products: structure, characterization, extraction and application-a review. *Polymers (Basel)*, 16(14).

Bello, K. A., & Maladzhi, R. W. (2025). Innovative and best practices in sustainable strategies for waste reduction in additive manufacturing. *Hybrid Advances*, 11(25), 1-11.

Blau, P. J. (2001). *Compositions, functions and testing of friction brake materials and their additives: a report by oak ridge national laboratory for U.S dept. of energy*. USA: U.S Dept. of Energy.

Croce, A., Bertolotti, M., Crivellari, S., Amisano, M., Nada, E., Grosso, F., Cagna, L., Rinaudo, C., Gatti, G., & Maconi, A. (2023). Scanning Electron Microscopy coupled with Energy Dispersive Spectroscopy applied to the analysis of fibers and particles in tissues from colon adenocarcinomas. *Working Paper of Public Health*, 11(1), 1-7.

Curado, A., Nunes, L. J. R., Carvalho, A., Abrantes, J., Lima, E., & Tomé, M. (2024). The use of asbestos and its consequences: an assessment of environmental impacts and public health risks. *Fibers*, 12(12), 1-14.

Dagwa, I. M., & Ibhadode, A. O. A. (2006). Determination of optimum manufacturing conditions for asbestos-free brake pad using Taguchi method. *Nigerian Journal of Engineering Research and Development*, 5(4): 1-8.

Ekpruke, E. O., Ossia, C. V., & Big-Alabo, A. (2023). Effects of grain size on the tribological performance of automotive brake pads from waste Thais Coronata shells. *Uniport Journal of Engineering and Scientific Research (UJESR)*, 7(2), 49-56.

Frank, A. L. (2020). Global use of asbestos - legitimate and illegitimate issues. *Journal of Occupational Medicine and Toxicology*, 15(16), 1-20.

Haruna, V. N., Abdulrahman, A. S., Abolarin, M. S., & Muriana, R. A. (2019). Evaluation of sheanut shell-reinforced automotive brake pad. *ARID Zone Journal of Engineering, Technology & Environment*, 15(3), 510-518.

Havlíček, Z., Novotná, I., Langová, L., Dostál, P., Votana, J., Dolezal, P., & Zabranský, L. (2025). Evaluation of hoof horn quality by tensile test and hardness test using acoustic emission. *Journal of Central European Agriculture*, 26(1), 13-21.

Hisam, M. W., Dar, A. A., Elrasheed, M. O., Khan, M. S., Gera, R., & Azad, I. (2024). The versatility of the Taguchi method: Optimizing experiments across diverse disciplines. *Journal of Statistical Theory and Applications*, 23(1), 365-389.

Idris, U. D., Aigbodion, V. S., Abubakar, I. J. & Nwoye, C. I. (2015). Eco-friendly asbestos free brake pad; using barana peels. *Journal of King Sand University-Engineering Services*, 27(8), 185 - 192.

Ikpambese, K. K., Gundu, D. T., & Tuleun, L. T. (2014). Evalution of palm kernel fibres (PKF) for production of asbestos - free automotive brake pads. *Journal of King Sand University - Engineering Sciences*, 120(1), 1- 9.

Irwan, A. P., Futriyana, D. F., Tezara, C., Siregar, J. P., Laksmidewi, D., Baskara, G. D., Abdullah, M. Z., Junid, R., Hadi, A. E., Hamdan, M. H. M., & Najid, N. (2022). Overview of the important factors influencing the performance of eco-friendly brake pads. *Polymers*, 14(6), 1-22.

Issa, A. K., Idris, M. H., & Tikau, M. I. (2020). Animal wastes as thermoplastic composite reinforcement materials for sustainable development. *International Journal of Innovative Technology and Exploring Engineering (IJITEE)*, 9(10), 62-66.

Mbakbaye, M. R., Ronoh, E. K., & Sanewu, I. F. (2021). Effects of shea nutshell ash on physical properties of lateritic soil. *SSRG International Journal of Civil Engineering*, 8(11), 1-6.

Montcho, M., Seidou, A. A., Nouri, B., Dao, A. N. C., Montcho, M., & Bougouma-Yameogo, V. (2025). Assessment and modeling of slaughterhouses waste sustainable management in west african cities: cases of main cities of Benin, Niger and Burkina Faso. *Waste and Biomass Valorization*, 1(1), 1-20.

Morăraș, C. I., Husaru, D., Goanță, V., Bârsănescu, P. D., Lupu, F. C., Munteanu, C., Cimpoesu, N., & Cosau, E. R. (2024). A new method for compression testing of reinforced polymers. *Polymers*, 16(21), 1-14.

Muhammed, K. O., Orilonise, A., Woli, T. O., Olatinwo, T. F., & Abdulazeez, M. A. (2024). Production and tribological evaluation of brake pad made from locally available materials. *International Journal of Information, Engineering & Technology*, 12(9), 61-69.

Nwankwo, E. I., Onyeananu, I. U., & Nwobi-Okoye, C. C. (2025). Bio-based brake pads: a review of natural fillers and their performance characteristics. *International Journal of Applied and Natural Sciences*, 3(2), 81-97.

Pradhan, T. R., & Shanti, S. K. (2023). A review on fabrication of recent novel brake friction materials. *International Journal of Recent Technology and Engineering (IJRTE)*, 12(2), 34-46.

Pujari, S., Ramakrishna, A., & Kumar, M. S. (2014). Comparison of jute and banana fibre composites: a review. *International Journal of Current Engineering and Technology*, (2): 121 - 129.

Ruzaidi, C. M., Kamarudin, H., Shamsul, J. B., & Abdullahi, M. M. A. (2011). Comparative study on thermal, compressive and wear properties of palm slag brake pad composite with other fillers. *Advanced Materials Research*, 341(342): 26 - 30.

Saraki, Y. A., Sulayman, F. A., & Sulaiman, I. (2025). Characterization and experimental analysis of aa7075 aluminium alloy and rice husk ash reinforced hybrid composite. *Arid Zone Journal of Engineering, Technology & Environment*, 21(1), 87-100.

Talabi, S. I., Ismail, S. O., Akpan, E. I., & Hassen, A. A. (2024). Quest for environmentally sustainable materials: A case for animal-based fillers and fibers in polymeric biocomposites. *Composites Part A: Applied Science and Manufacturing*, 183(1), 1-15.

Umamaheswara, R. R., & Babji, G. (2015). A review paper on alternate materials for asbestos brake pads and its characteristics. *International Research Journal of Engineering and Technology (IRJET)*, 2(2), 556-562.

Ushie, A. P., Paschal, U. A., Abdulrahman, S. A., & Oyeyemi, S. W. (2024). Investigation of mechanical properties of cow bone and poultry feather reinforced rldpe composites for sustainable material applications. *FUDMA Journal of Sciences (FJS)*, 8(6), 211 - 216.

Yawas, D. S., Aku, S. Y. & Amaren, S. G. (2016). Morphology and Properties of Periwinkle Shell Asbestos Free Brake Pad. *Journal of King Saud University-Engineering Sciences*, 28(1), 103 - 109.

Zievie, P., Yalley, P., Danso, H., & Antwi, K. (2024). Utilisation of Waste shea nutshell fine-grained particles to enhance strength and durability behaviour of concrete . *International Journal of Engineering Materials and Manufacture*, 9(2), 1-5.